Performance assessment of pulse blanking mitigation in presence of multiple Distance Measuring Equipment/Tactical Air Navigation interference on Global Navigation Satellite

Published in IET Radar, Sonar and Navigation
Received on 3rd July 2013
Revised on 3rd October 2013
Accepted on 20th October 2013
doi: 10.1049/iet-rsn.2013.0198

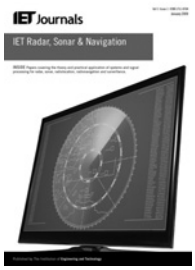

ISSN 1751-8784

Performance assessment of pulse blanking mitigation in presence of multiple Distance Measuring Equipment/Tactical Air Navigation interference on Global Navigation Satellite Systems signals

Luciano Musumeci[1], *Jaron Samson*[2], *Fabio Dovis*[1]

[1]*Department of Electronics and Telecommunications, Politecnico di Torino, Turin, Italy*
[2]*Radio Navigation Systems and Techniques (TEC-ETN), European Space Agency ESA/ESTEC, Noordwijk, The Netherlands*
E-mail: luciano.musumeci@polito.it

Abstract: It is known that the Aeronautical Radio Navigation Systems sharing the Global Navigation Satellite Systems (GNSS) frequency band represent a threat to the satellite-based navigation services. Distance Measuring Equipment (DME) and Tactical Air Navigation (TACAN) systems broadcast strong pulsed ranging signals within the Global Positioning System L5 and Galileo E5a frequency bands where the aviation positioning aids services are allocated. This study provides an experimental assessment of the DME/TACAN interference effect on the GNSS receivers performance in scenarios where the presence of several transmitters in view generates radio-frequency interference hard to mitigate by means of the classical solutions. In detail, analysis in terms of the receiver performance will be presented by showing the effect of the non-ideal pulse blanking on the GNSS signal quality. The optimal set-up of the mitigation process, investigated by means of a software simulation, is provided.

1 Introduction

As a result of the modernisation process of the Global Positioning System (GPS) together with the new four Galileo In-Orbit-Validation satellites, successfully placed in their respective orbits [1, 2], a new set of Global Navigation Satellite Systems (GNSS) frequency bands is now available: GPS L5 and the Galileo E5. These new signals are becoming quite attractive for the GNSS community because of the fact that new modulation schemes are employed as for example the Alternative Binary Offset Carrier (AltBOC(15,2)) in the E5 frequency bands. The constant envelope of the AltBOC modulated signals could lead to excellent performance for those GNSS high-end receivers able to process the entire Galileo E5 frequency bands. Moreover, the GPS L5 and the Galileo E5 frequency bands will be devoted to the civil transportation field as the Aeronautics community where accurate, precise and reliable positioning information are needed especially during the landing operation of the civilian aircraft.

Nevertheless, for the GNSS-based aviation services, a very harsh interference environment is expected, as described, for example, in [3]. In fact the GPS L5 and the Galileo E5 frequency bands are shared with other aero-radio navigation systems which broadcast aiding navigation information through pulsed ranging signal transmission, such as the Distance Measuring Equipment (DME) and the military Tactical Air Navigation (TACAN). In this scenario, the most common interference mitigation algorithm against pulsed interference employed is the pulse blanking. The aim of this paper is to provide an exhaustive description of the potential effects of the DME/TACAN interference on the GNSS received signal quality and on GNSS receiver performance when multiple interference sources are present, and pulse blanking is used to mitigate their effect. The analysis is supported by a set of experimental tests performed at the navigation laboratory of the European Space Research and Technology Centre (ESTEC) which will be provided. The benefits and the drawbacks of this interference mitigation technique will be assessed by means of software simulations, considering both ideal and non-ideal pulse blanking. Ideal and non-ideal pulse blanking effects have been already addressed in [4, 5], considering the presence of one single rectangular pulse. In this paper, the blanking operation will be investigated in the presence of composite pulsed interference assessing the performance degradation and optimising the parameters of the blanker for a given scenario. The paper is organised as follows. Section 2 will recall the main features of the DME/TACAN systems, and Section 3 will summarise the features of the pulse blanking mitigation. Sections 4 and 5 will then analyse the multiple DME/TACAN interference scenarios theoretically and by simulation, respectively. Finally, in Section 6, a performance comparison between the ideal and the non-ideal pulse blanking mitigation will be provided by means of a software simulation, in order to optimise the blanker parameters.

2 DME/TACAN systems

The DME and the TACAN systems provide slant range information between an aircraft and an equipped ground reference station. Both the systems are based on the communication between two components, one installed onboard the aircraft (interrogator) and another one placed on the ground (transponder). The interrogator sends a request to the DME/TACAN ground stations broadcasting towards the ground a pulse pair sequence; the ground beacons reply to the received pulse pair sequence with the same pulse pair sequence delayed of 50 μs towards the sky, thus allowing the onboard DME/TACAN receiver to compute the slant range measurement based on a round trip time measurement.

The DME/TACAN operates in four different modes (X, Y, W and Z) each of which identifies a different method of coding the pulse pair transmissions by time spacing pulses within a pulse pair, but only the X-mode replies that are transmitted in the frequency range 1151–1213 MHz, are a real threat for the onboard GNSS receivers. These replies are made of pulse pair sequences where each pulse duration is equal to 3.5 μs and the spacing between the pulse pairs is 12 μs. These trains of pulse pairs are transmitted from the ground station with a maximum pulse repetion frequency (PRF) equal to 2700 pulse pair per second (ppps) for the DME and 3600 ppps for the TACAN, when a maximum of 100 aircraft have to be served. Concerning the pulse power, the maximum Equivalent Isotropic Radiated Power transmitted by the DME/TACAN ground beacons is 40 dBW. Thus, the DME/TACAN pulse power reaching an onboard antenna at high altitude but still within the maximum coverage range of a ground station (about 519 km), is quite higher than the GNSS signal power level. Additional specifications of both the systems can be found in [6].

3 Pulse blanking

In Fig. 1, the modulated and normalised DME/TACAN double pulse is represented. As it is clear from the left side plot of Fig. 1, the DME/TACAN pulse can be modelled as a modulated Gaussian shaped pulse, as proposed in [7]. Based on this Gaussian shape assumption, the DME/TACAN signal is

$$s_{\mathrm{DME/TACAN}}(t) = \sqrt{\left(J \cdot |H(f_{\mathrm{J}})|^2\right)} \sum_k \left(\mathrm{e}^{\left(-\alpha(t-t_k)^2/2\right)} + \mathrm{e}^{\left(-\alpha(t-\Delta t-t_k)^2/2\right)} \right) \times \cos\left(2\pi\left(f_{\mathrm{IF}} + \Delta f_{\mathrm{jammer}}\right)t + \theta_{\mathrm{J}}\right) \quad (1)$$

where J is the pulse peak power at the antenna port, f_{J} is the received jammer carrier frequency, t_k is the ensemble of the pulse pairs arrival times, $\Delta f_{\mathrm{jammer}}$ is the frequency offset between the jammer carrier with respect to the Galileo E5a or the GPS L5 carrier frequency, θ_{J} is the jammer carrier phase and α is a parameter of the DME/TACAN pulse equal to 4.5×10^{11} s^{-2}. The most traditional countermeasure adopted against the pulsed interference is the pulse blanking, implemented by means of a circuit in the digital part of the receiver front-end. Such a technique performs an interference excision in the time domain by thresholding sample by sample the output of the analogue-to-digital converter (ADC), as shown in Fig. 1. The pulse detection in this case can be performed in either analogue circuitry, through analogue power measurement, or digital circuitry, looking at the histogram of the samples at the output of the ADC [8].

This simple mechanism offers good performance in suppressing the pulsed interference especially in those interference scenarios where the pulsed signals are not so dense in time because of the presence of a limited number of sources of pulsed signals. This is not the case with the DME/TACAN interference experienced by an onboard receiver at high altitude. In many real scenarios, the pulse blanking circuitry is triggered by the composite strong pulsed signals reaching the onboard GNSS receiver antenna, causing the suppression of large portions of the useful GNSS signal power together with the interference power, thus increasing the probability to fail the acquisition and tracking of the signal itself [9].

Moreover, the pulse blanking circuit performance can be negatively influenced by the effect of the pulsed signals on the other components in the receiver front-end. Very strong

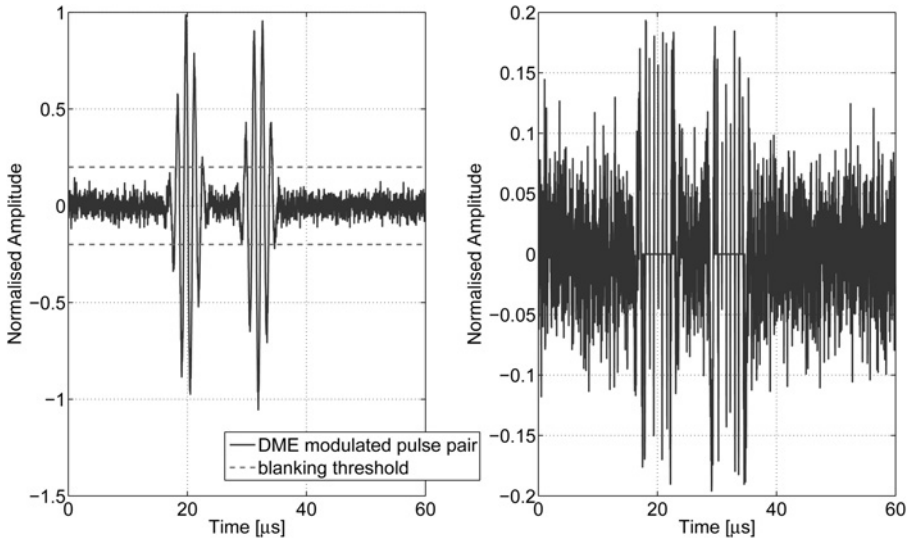

Fig. 1 *Ideal pulse blanking operation on a DME/TACAN pulse pair*

doi: 10.1049/iet-rsn.2013.0198

pulses or very strong received power because of the combination of multiple pulses can cause the saturation of the active components in the GNSS receivers (e.g. amplifiers), which may require a 'recovery' time to go back to a normal state when the interference ends. In [4] it is mentioned that for a particular commercial receiver, an interference pulse signal with peak power 15 dB above the thermal noises is sufficient to saturate the last amplification stage within the receiver front-end. The multiple DME/TACAN interference scenario that will be introduced later is composed of pulsed signals with pulse peak power 20 dB above the thermal noise. Under this interference environment condition, pulse blanking may perform signal suppression even during the off state of the pulse for a time period similar to the 'recovery' time needed by the amplifiers to resume normal operation. For a commercial receiver, typical 'recovery' times for the amplification stages are about 40 ns/dB of input level beyond the saturation point [4]. In general, the impact of pulsed interference signals on the receiver front-end components might be different depending on the pulse peak power level and the pulse duration. Furthermore, the automatic gain control (AGC) is needed when the multibit quantisation is implemented in the digital part of the receiver front-end. The AGC is in charge to properly set the amplitude dynamic of the ADC input signal. A slow AGC set the A/D input levels averaging the input signal power over a large time during which, if too many pulses oscillations are present, the input dynamics of the ADC is not properly set [4]. We also have to consider the fact that the blanked samples should not be use for the AGC tuning in order to avoid ADC overloading. Owing to these several reasons, the blanking operation might not be efficient, since a high percentage of the received signal may be blanked [5]. Fig. 1 shows also that not all the samples belonging to the pulse are suppressed because of the presence of the modulation over the pulse duration and to the truncated Gaussian shape of the single DME/TACAN pulse, leading to an increased noise floor [7]. It is clear that all these effects are amplified for the receivers operating in a scenario affected by a large number of DME/TACAN stations thus leading to unacceptable performance of the GNSS systems onboard. This kind of scenario has been addressed in [10], where a wavelet-based technique has been proposed for the pulsed interference suppression. In this paper, we consider the optimisation of the classical blanker parameters in order to deal with the multiple pulses.

The blanking threshold determination is not a trivial operation. Typical values of blanking threshold are included within 5 and 10 dB above the noise power, but the real hardware receivers are equipped with a pulse blanking circuit with a variable blanking threshold which changes according to the received signal quality. One of the criteria used for the blanking threshold determination is based on the statistical properties of the GNSS signal distribution at the output of the ADC in an interference-free environment. Since the GNSS received signal is completely buried in the noise floor, the distribution of the samples at the ADC output can be modelled as Gaussian distributed. Thus, based on the so called Neyman–Pearson criteria, the blanking threshold is chosen according to a required false alarm probability p_{fa}, which can be expressed as follows

$$p_{\text{fa}} = 2 \cdot \int_{V_{\text{th}}}^{\infty} f_{\text{s}}(x)\, \text{d}x = \text{erfc}\left(\frac{V_{\text{th}}}{\sigma\sqrt{2}}\right) \tag{2}$$

where V_{th} is the blanking threshold and σ is the standard deviation of the samples at the front-end output. Thus, the blanking threshold level is determined as

$$V_{\text{th}} = \sigma\sqrt{2} \cdot \text{erfc}^{-1}\left(p_{\text{fa}}\right) \tag{3}$$

This criterion will be considered in the remainder of the paper.

4 Multiple DME/TACAN interference scenario

4.1 Theoretical model

In the literature, the effect of a pulse blanking circuit on the GNSS receiver performance has been widely investigated. A theoretical model for computing a prediction of the pre correlator C/N_0 in the presence of strong and dense in time DME/TACAN interference is presented in [8] and [11]

$$(C/N_{0,\text{eff}}) = \frac{C}{N_0} \cdot \frac{(1-\beta)}{1 + (I_{0,\text{WB}}/N_0) + R_I} \tag{4}$$

where β, representing the blanker duty cycle, is the total mean activation time of the blanker and R_I is the aggregate post-correlator ratio between the residual DME/TACAN power, after the blanker, and the receiver thermal noise. The residual DME/TACAN power is generated by all the pulses' samples below the blanking threshold, that contribute to increase in the noise floor.

To assess the theoretical value of the $C/N_{0,\ \text{eff}}$ for the scenarios that have been analysed in this work, the values of β and R_I have to be obtained based on the derivation in [7, 12].

(1) *β computation:* The total mean activation time β of the blanker is determined by all the pulses whose peak power is above the blanking threshold. In [7], the mean activation time of a blanker under strong DME/TACAN interference is defined as

$$\beta = 2 \cdot \left(\sum_{i=1}^{N} \text{PRF}(i)_{\text{DME}} \cdot T_{m,\text{DME}}(i)\right) + 2 \cdot \left(\sum_{i=1}^{M} \text{PRF}(i)_{\text{TACAN}} \cdot T_{m,\text{TACAN}}(i)\right) \tag{5}$$

where PRF is the pulse repetition frequency of each ground station while T_m is the blanker activation time for one single strong pulse, in the presence of different possible collision scenarios. The mean activation time of the blanker in the presence of one strong pulse without any pulse superposition and assuming a Gaussian shape for the pulse, is defined as

$$T = 2 \cdot 2\sqrt{\frac{\ln\left(P_{\text{strong}}/V_{\text{th}}\right)}{\alpha}} \tag{6}$$

where V_{th} is the blanking threshold power and P_{strong} is the pulse peak power. Thus, by modelling the pulses arrival to the GNSS onboard the receiver as a Poisson process, and by taking into account the modulation over the pulse duration, the blanker activation time for one single strong

doi: 10.1049/iet-rsn.2013.0198

pulse becomes T_m in the presence of different collision scenarios

$$T_m = \gamma\left(\frac{J}{\text{th}}\right) \cdot \left(T\mathrm{e}^{-\lambda T} + \frac{T}{2}\frac{(\lambda T)}{1!}\mathrm{e}^{-\lambda T} + \frac{T}{3}\frac{(\lambda T)^2}{2!}\mathrm{e}^{-\lambda T} + \cdots\right) \quad (7)$$

where γ is a reduction factor dependent on the ratio between the pulse peak power J and the blanking threshold V_{th}. Additional details on this theoretical model can be found in [7].

(2) *R_I calculation:* R_I is defined as

$$R_I = \frac{1}{N_0 \cdot \text{BW}} \cdot \sum_{i=1}^{N} P_i \cdot \text{dc}_i \quad (8)$$

where N is the total number of the DME/TACAN sources; P_i is the received peak power of the ith RFI pulsed signal source; BW is the pre correlator IF bandwidth and dc_i is the duty cycle of the ith signal source without any pulse collision. We refer to the model in [7, 12] where R_I is defined as splitting the contribution of the strong and the weak DME/TACAN signals. The weak pulsed signal (with the peak power below the blanking threshold) will contribute with their total power to the interfering power. Equation (8) can then be elaborated as

$$\begin{aligned} R_I &= \frac{1}{N_0 \cdot \text{BW}} \cdot \sum_{i=1}^{N} P_i \cdot \text{dc}_i \\ &= \frac{1}{N_0 \cdot \text{BW}} \cdot \left(\sum_{j=1}^{M} P_{\text{strong},j} \cdot \text{dc}_{\text{residual},j}\right) \\ &\quad + \frac{1}{N_0 \cdot \text{BW}} \cdot \left(\sum_{k=1}^{L} P_{\text{weak},k} \cdot \text{dc}_{\text{weak},k} \cdot \text{SSC}_{\text{weak},k}\right) \end{aligned} \quad (9)$$

where the spectral separation coefficient is introduced as the weighting factor for those DME/TACAN signals whose peak power is below the blanking threshold. In [7, 12], a rectangular equivalent pulse width of 2.64 μs is used for modeling the contribution to the noise floor caused by the weak DME/TACAN pulses. Thus, the duty cycle for the weak DME/TACAN signals can be written as

$$\text{dc}_{\text{weak},k} = 2 \times 2.64\ \mu\text{s} \cdot \text{PRF}_{\text{weak},k} \quad (10)$$

where $\text{PRF}_{\text{weak},\,k}$ is the pulse repetition frequency of the kth weak DME/TACAN signal.

Regarding the contribution because of the strong DME/TACAN pulses (with the peak power over the blanking threshold), from (6) the residual portion of the samples below the threshold belonging to the pulse pair is

$$\text{PW}_{\text{residual}} = 2\sqrt{\pi/\alpha} \cdot \text{erfc}\left(\sqrt{\ln\left(P_{\text{strong}}/V_{\text{th}}\right)}\right) \quad (11)$$

Then, the duty cycle for the residual portion of the strong DME/TACAN signals which contributes to the noise floor becomes

$$\text{dc}_{\text{residual},j} = \text{PW}_{\text{residual},j} \cdot \text{PRF}_{\text{strong},j} \quad (12)$$

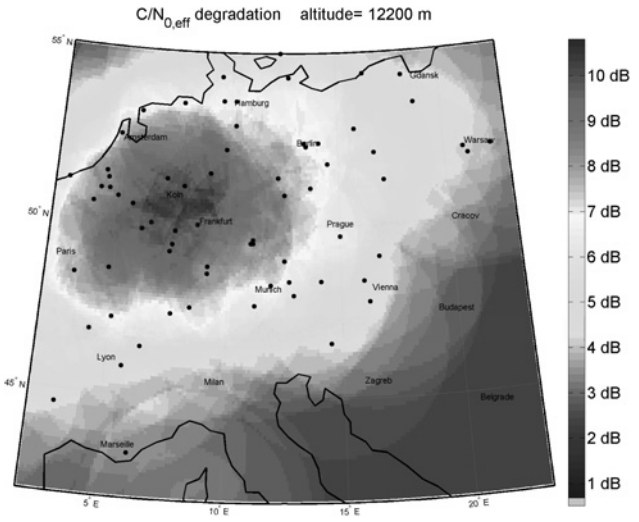

Fig. 2 *Carrier-to-noise density ratio degradation prediction over Europe*

4.2 Case study of central Europe

By using the theoretical model so far described, a prediction of the C/N_0 degradation because of the DME/TACAN signals has been performed for a grid of locations at 40 000 feet over Europe. For this simulation real DME/TACAN ground beacons, transmitting within the GPS L5 and the Galileo E5a frequency bands, have been taken into account and for each of them the maximum PRF has been considered. Moreover, both the DME/TACAN beacons pattern antenna defined in [12] and the GNSS typical aircraft antenna pattern have been simulated in order to perform an accurate calculation of the received pulsed interference level power at the GNSS onboard antenna. It is worth outlining that no aircraft body attenuation has been taken into account.

Fig. 2 shows the profile of the predicted post-correlator C/N_0 degradation caused by the composite DME/TACAN signals coming from all the DME/TACAN ground stations represented by the black dots. For this simulation, an analogue power level 2.5 dB over the noise power level, has been used as the blanking threshold, fixed according to a false alarm probability of 10^{-2}. The worst location in terms of the C/N_0 degradation is identified for a latitude of 50, 7° and for a longitude of 8, 9° at an altitude of 40 000 feet. At this location, roughly corresponding to the area over the Frankfurt airport, the GNSS receiver operation might be corrupted by the composite pulsed signal coming from up to 40 DME/TACAN stations broadcasting within the GPS L5 and the Galileo E5a frequency bands. Under this simulated interference environment, the blanking circuit cuts off about 56% of the total GNSS received signal, thus producing a degradation on the $C/N_{0,\,\text{eff}}$ of about 10.2 dB.

Fig. 3 shows the trend of the $C/N_{0,\,\text{eff}}$, the blanker duty cycle β and the factor R_I with respect to the value of the blanking threshold, simulated at the 'DME/TACAN hotspot location' previously identified. As expected, Fig. 3*a* shows that the blanker duty cycle β is decreasing with the increasing of the blanking threshold, whereas the degradation on the $C/N_{0,\,\text{eff}}$ has an optimum point. This is due to the fact that a low blanking threshold would increase the percentage of the signal being blanked while a higher blanking threshold would cut off a minor percentage of the received signal, allowing the majority of the pulsed interference to go through the correlator, increasing the

doi: 10.1049/iet-rsn.2013.0198

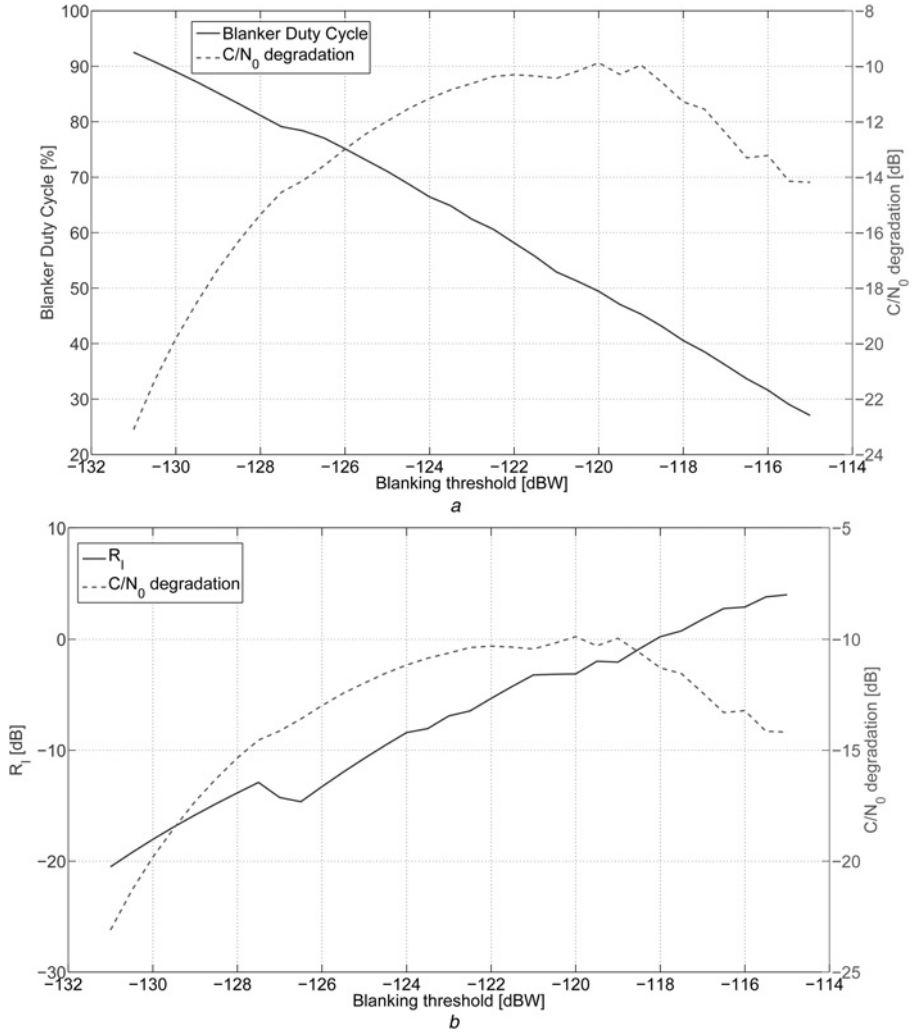

Fig. 3 *Blanker duty cycle β and R_I factor against the blanking threshold*

a Blanker duty cycle β and C/N_0 degradation versus the blanking threshold variation
b Pulsed interference contribution to the noise floor (R_1) and C/N_0 degradation versus the blanking threshold variation

noise floor because of an increased R_I contribution, as can be observed in Fig. 3*b* where the factor R_I is plotted against the blanking threshold. Thus, a careful design of the blanking circuit has to be performed in order to achieve the best trade-off between the percentage of the signal blanked and the $C/N_{0,\,\mathrm{eff}}$ degradation.

The analysis performed in this case study, shows that the blanking threshold should be optimised, in order to avoid unacceptable drops in the C/N_0 because of the presence of multiple interfering pulses. Moreover, an a priori optimisation of the threshold value by the simulation requires a large amount of details of the DME and the TACAN ground stations, thus making this task not easy to accomplish.

5 Experimental simulation of the multiple DME/TACAN interference scenario

To validate the results based on the theoretical model, a test campaign has been performed at the ESTEC navigation laboratory by using the powerful Interference Test Facility (ITF). The ITF is a hardware software platform capable of generating a wide range of realistic interference scenarios and it is mostly devoted to the testing of the GNSS hardware receiver performance under interference. More details on the different capabilities and the configurations of this tool can be found in [13].

A Spirent GNSS constellation simulator and signal generator as well as an Agilent signal generator have been used. They are connected to an Ethernet network together with a desktop PC hosting the software managing the ITF. Through this network connection, both the Spirent and the Agilent generators have been driven remotely from the ITF Human Machine Interface. The latest release of the ITF software provides the possibility to generate a wide range of realistic DME/TACAN interference environments by a proper setting of the parameters as the number of ground beacons to simulate, the carrier frequency and pulse repetition frequency for each simulated beacon, pulse width and inter pulses spacing, pulse peak power for each DME/TACAN signal and finally a time offset between all the different DME/TACAN signals in order to simulate the pulses' arrival time to the onboard GNSS antenna.

Then, the composite DME/TACAN interference is combined with the GNSS signal generated by the Spirent at Radio-Frequency. Eventually, the composite GNSS signal interfered by the DME/TACAN signals has been fed to an RF splitter, the outputs of which have been connected with a Tektronix Spectrum Analyser and a hardware Test User Receiver (TUR), respectively.

doi: 10.1049/iet-rsn.2013.0198

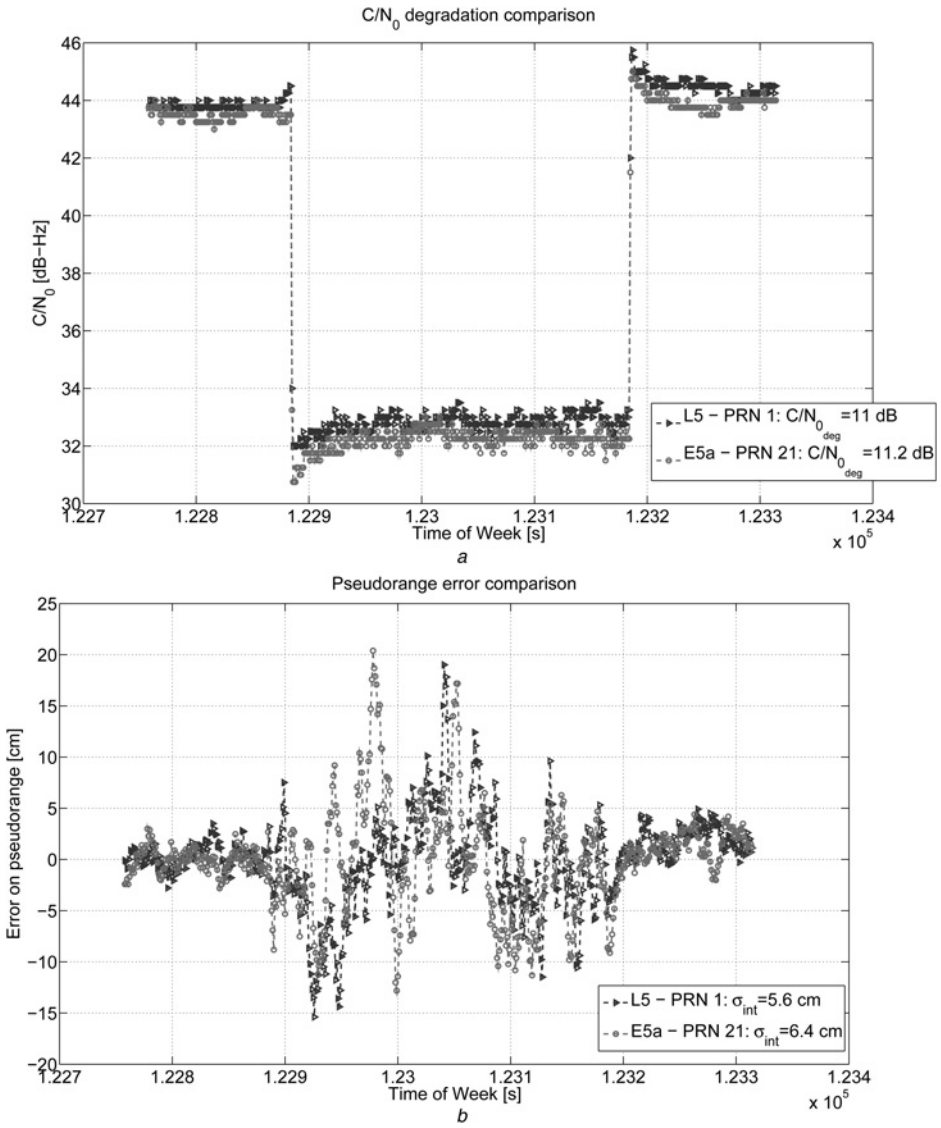

Fig. 4 *TUR performance under the DME/TACAN interference in the Galileo E5a and the GPS L5 frequency bands*

a TUR C/N_0 estimation in the GPS L5 and Galileo E5a frequency bands during the test duration
b TUR pseudorange error in the GPS L5 and E5a frequency bands during the test duration

The GPS L5 and the Galileo E5a signals have been generated with a power level such that the pre-correlator carrier-to-noise density ratio estimated by the TUR receiver is equal to 44 dB-Hz for both signals in an interference-free environment.

Fig. 4 shows the TUR receiver performance in tracking the Galileo E5a and the GPS L5 signals (PRN 21 and 1, respectively), under the DME/TACAN interference environment considered. In particular, Fig. 4*a* provides comparison between the $C/N_{0,\ meas}$ estimated by the TUR receiver in both the Galileo E5a and the GPS L5 frequency bands, during all the test durations. As soon as the DME/TACAN signal is injected in the setup, a drop on the $C/N_{0,\ meas}$ of about 11 dB is observed in both the figures, and the blanker duty cycle value during all the interference period is around 56%. Such a value of degradation is approximately 1 dB far from the theoretical value estimated by using the model and that can be observed in Fig. 3*a*. Furthermore, according to Fig. 3*a*, in correspondence of a blanker duty cycle β of 56%, a blanking threshold level power of −121.5 dBW can be observed and assumed as a potential equivalent blanking threshold for the TUR blanker circuitry. Despite a large portion of the signal being cut off by the blanking circuit, the TUR receiver is still able to keep the tracking of both the GNSS signals, computing a pseudorange measurement affected by an increased error as shown in Fig. 4*b*.

Fig. 5 shows the effect of the DME/TACAN interference on the different satellites. A typical GNSS aviation pattern antenna has been simulated by enabling the antenna pattern options from the Spirent generator. The upper plot shows the $C/N_{0,\ meas}$ estimated by the TUR receiver for each E5a PRN tracked during all the test durations, whereas the plot on the bottom shows the trends of the geometric dilution of precision (GDOP) (dashed line) and the number of satellites used by the TUR in the GDOP computation (continuous line). Since a GNSS aviation pattern antenna is simulated, the GNSS signals coming from the satellites at low elevation are tracked with a lower initial $C/N_{0,\ meas}$. Once the DME/TACAN interference is injected into the setup, the TUR receiver immediately loses track of the weakest GNSS signals, thus affecting the GDOP as shown in the bottom plot. During the interference-free period, a good GDOP value was computed on the basis of six satellites, whereas during the interference period only four satellites were used

doi: 10.1049/iet-rsn.2013.0198

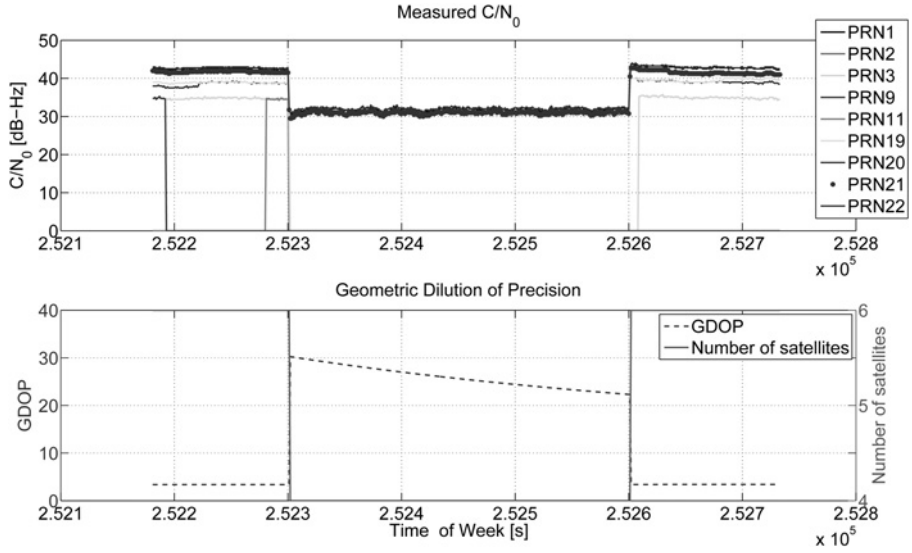

Fig. 5 *DME/TACAN interference effect on the C/N_0 and the Geometric Dilution of Precision*

for the fix. A great increase on the GDOP value is observed when the TUR receiver is under the DME/TACAN interference, thus affecting the final position computation.

This test campaign revealed that the DME/TACAN interference in some cases might be a disruptive interference even if the GNSS receiver is equipped with a blanker which is forced to cut off great portions of the useful signal, as proved by the blanker duty cycle β provided by the receiver. Great losses on the $C/N_{0,\ \mathrm{meas}}$ might lead the receiver to losing the tracking of the feeble GNSS received signals, thus affecting the final user position accuracy, worsening both the quality of the pseudorange and the GDOP factor.

It has to be mentioned that no information on the TUR receiver front-end design, blanking circuitry and blanking threshold setting criteria is available. Such missing information does not allow us to find out if the non linearities effect on the pulse blanking are excited by the saturation of the AGC.

Thus, parametric software simulations considering both the ideal and the non-ideal pulse blanking mitigation in the presence of multiple DME/TACAN interferences have been tested and presented in the next section.

6 Pulse blanking assessment in multiple DME/TACAN interference: a software implementation

Ideal and non-ideal pulse blanking have been both software implemented and applied on a set of data collected at intermediate frequency and interfered with the multiple DME/TACAN interference presented in Section 4 and simulated in the experimental test described in Section 5. The purpose of this test campaign, performed by means of a full software simulation, is to investigate if the DME/TACAN multiple interference scenario, so far described, may generate non-linear effects within the employed TUR receiver front-end, thus leading to a non-ideal behaviour of the TUR pulse blanking circuitry.

6.1 Front-end setup

A set of data collections at intermediate frequency have been performed by using a discrete components front-end. The considered front-end has been used in the same hardware setup configuration described in Section 5, connecting one of the outputs of the RF splitter at its input. Such a front-end is characterised by two amplification stages followed by a down-conversion to an intermediate frequency of 225 MHz. Additional amplification stages followed by a final filtering stage with an 18 MHz IF filter bandwidth produced the output signal for the ADC where the signal is sampled at 36 MHz and quantised over 8 bits. A USB interface integrated in the front-end is in charge of transferring the quantised samples from the ADC to a user terminal where a data grabber software is installed. It has to be remarked that no AGC is implemented in the considered device and the embedded stages have been designed such that the ADC saturation is avoided in the presence of the DME/TACAN interference. Moreover, all the amplification stages are realised with the amplifiers which allow input level power up to 10 dBm, thus avoiding any saturation effects within the receiver front-end. The principles for the GNSS receiver front-end design can be found in [14].

Unlike the ideal blanking mechanism, which provides suppression of all and only the samples exceeding a predetermined threshold level power, in the non-ideal blanking software implementation algorithm, a suppression of an amount of the samples below the blanking threshold after the theoretical deactivation of the blanker, is implemented. This blanking latency is introduced in order to model the cumulative effect of the 'recovery' time required by the amplifiers within the receiver front-end after the saturation condition. It is important to mention that the amplifiers and the ADC saturations introduce non-linearity in the composite received signal at the input of the digital pulse blanker, since the pulse interference cannot be considered additive to the GNSS received signal.

6.2 Recovery time

The first performed simulation aims at assessing the effect of the recovery time on the pulse blanking performance. The deactivation delay of the blanking algorithm is simulated by suppressing a certain number of the samples below the blanking threshold after the ideal blanker deactivation instant. As a consequence, a certain amount of samples

doi: 10.1049/iet-rsn.2013.0198

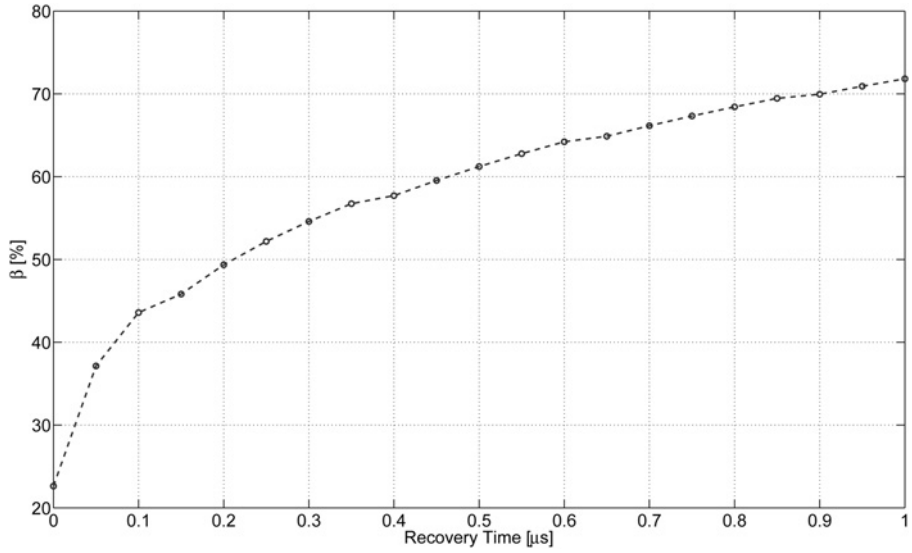

Fig. 6 *Blanker duty cycle against recovery time*

belonging to the tails of the composite pulses are also suppressed. The range of values that has been considered for the recovery time are comprised within 0 and 1 μs and the blanking threshold level employed in the software implemented pulse blanker, has been set according to a false alarm probability p_{fa} equal to 10^{-2} for a proper fair comparison with the experimental results obtained in Section 5. The results are shown in Fig. 6. Considering the results obtained in Section 5, under the same DME/TACAN interference environment, the percentage of the signal blanked by the pulse blanking circuitry implemented in the TUR was about 56% which in Fig. 6 corresponds to a recovery time of about 0.4 μs. Such a value is likely because of the strong DME/TACAN interference that saturates the amplification stages of the hardware receiver used in the test campaign thus affecting the pulse blanking performance. A better design of the front-end, avoiding the saturation status and a consequential reduction of the recovery time, could reduce the performance loss, as described in the next section.

6.3 Pulse blanking optimisation in the presence of the DME/TACAN interference

The simulation results obtained in Section 6.2 showed that the pulse blanker of the prototype receiver used during the test campaign at the ESTEC may have a non-ideal behaviour under strong DME/TACAN interference. The DME/TACAN power level at the onboard receiver antenna is strong enough to generate the non-linear behaviour of some active components within the receiver front-end. In this section, a parametric assessment of the non-perfect blanking operation on the GNSS receiver performance is presented. The non-ideal blanking operation has been software implemented and applied off-line to a dataset collected at intermediate frequency under the strong multiple DME/TACAN interference scenario described in Section 5. Recovery time values in the range 0–1 μs have been considered for the software application of a non-ideal blanking operation on the interfered dataset. A fully software GNSS receiver, N-GENE [15], has been exploited

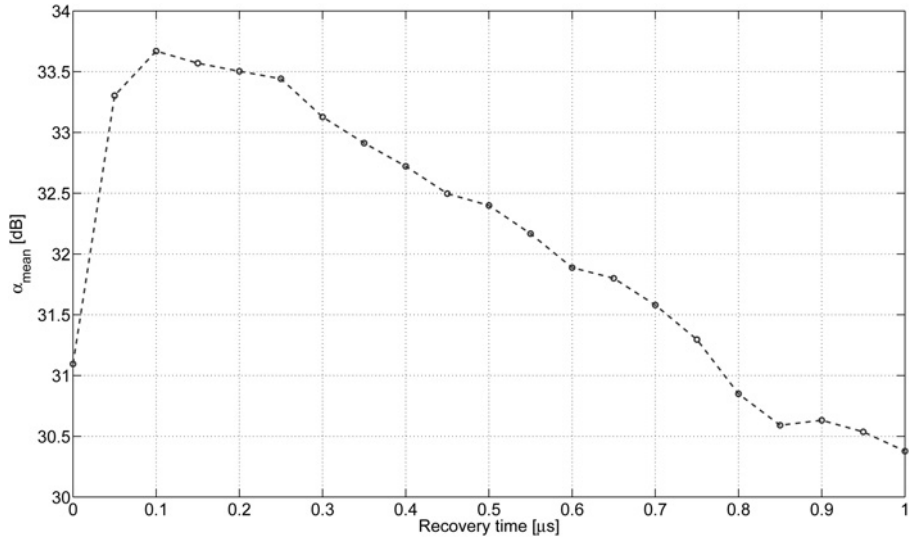

Fig. 7 *Acquisition metrics against recovery time*

doi: 10.1049/iet-rsn.2013.0198

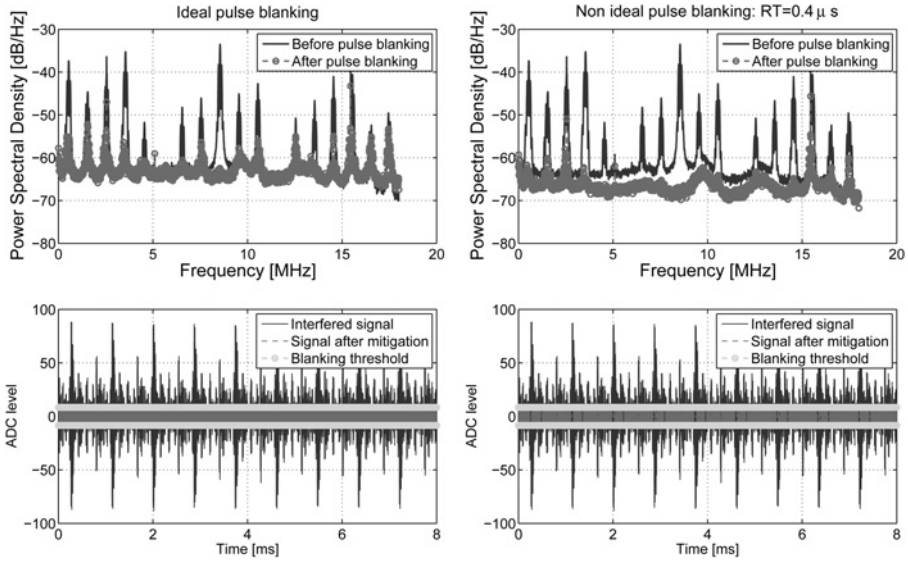

Fig. 8 *Time and frequency signal representations comparison: ideal blanking against non-ideal blanking*

in order to assess the effect of the non-ideal blanking behaviour at the acquisition level. The figure of merit

$$\alpha_{\text{mean}} = \frac{R_p}{M_c} \tag{13}$$

which is the ratio between the main peak and the noise level of the correlation floor has been considered.

For each considered value of the recovery time, a software blanking operation has been performed leading to the generation of different datasets which have been fed to the acquisition processing block of the N-GENE software receiver. The results are shown in Fig. 7, where the acquisition metrics α_{mean} is reported as a function of the recovery times simulated in the non-ideal blanking software implementation.

In this figure, three different regions can be identified:

- *Ideal blanking region* in correspondence of a null recovery time, where the acquisition metric α_{mean} reaches 31.1 dB.
- *Optimal blanking region* between 0.05 and 0.75 μs for the recovery time, where the interference suppression leads to acquisition metric values higher than the acquisition metric obtained through a perfect blanking. Within this region of the recovery times values, the percentage of the suppressed interference signal power is higher than the percentage of the suppressed useful signal power.
- *Degraded blanking region* over 0.75 μs for the recovery time, where the interference cancellation leads to worse acquisition metrics with respect to the performance achieved through a perfect blanking.

On conclusion, it is possible to identify a precise point in correspondence of a recovery time equal to 0.1 μs where the acquisition metric α_{mean} reaches the value of 33.6 dB. This point can be considered as an optimal working point for the pulse blanking circuit, in such a DME/TACAN scenario.

In Section 6.2, an equivalent cumulative recovery time equal to 0.4 μs has been identified by means of a software simulation for the prototype receiver employed during the

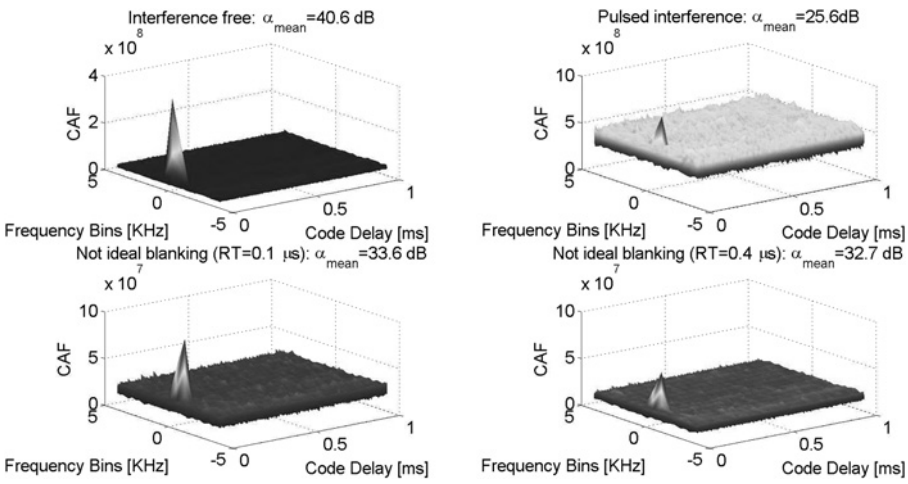

Fig. 9 *Galileo E5a-Q PRN 20 Acquisition search spaces*

doi: 10.1049/iet-rsn.2013.0198

test campaign described in Section 5. Fig. 8 shows the time and the frequency behaviour of the signal before and after, respectively, ideal pulse blanking (left plots) and non-ideal pulse blanking (right plots). Concerning the frequency domain, the plot on the top left corner shows that after an ideal blanking operation, several narrow band (380 kHz) jamming components with peak powers ranging from 20 up to 35 dB over the GNSS received signal power level are reduced but still visible, while the plot on the top right corner shows that, because of the latency of the blanker, more interference power as useful signal power is suppressed. This is also confirmed by looking at the time representation of both the signals before and after pulse blanking. In the bottom right plot, the signal after the non-ideal pulse blanking (dashed line) results is more suppressed with respect to the signal after an ideal blanking operation (bottom left corner).

Figure 9 shows the acquisition search spaces obtained by means of the N-GENE software receiver in the following cases, in clockwise position:

- Interference-free scenario.
- Pulsed interfered scenario.
- After pulsed suppression through the optimal blanker (recovery time of 0.1 μs).
- After pulsed suppression through the non-ideal blanking considering a recovery time of 0.4 μs.

1 ms of coherent integration time and 100 non-coherent accumulations allows the acquisition of the E5a pilot channel even in the presence of the strong DME/TACAN interference leading to an acquisition metric α_{mean} equal to 25.6 dB. The results confirm that the use of the pulse blanking provides interference suppression thus improving the acquisition receiver performance. α_{mean} grows up to 33.6 dB when an optimal blanker in terms of recovery time (0.1 μs) is employed.

7 Conclusions

The experimental results presented in the paper show that the DME/TACAN interference may constitute a disruptive interference for the onboard GNSS receiver flying at high altitude (40 000 ft). In such a scenario, the DME/TACAN interference is composed of all the DME/TACAN pulse signals coming from several ground stations in the line of sight with the onboard GNSS antenna, thus resulting in a pulsed interference environment extremely dense in time. Even in the presence of a traditional interference countermeasure as the pulse blanking, the GNSS hardware receiver operation might be compromised, since great portions of the incoming signal are suppressed by the blanker circuitry, thus leading to a considerable degradation of the incoming GNSS signal at the input of the receiver baseband processing block.

These results have shown that the pulse blanking performance is strongly dependent on the GNSS receiver architecture. In particular, the designs of the amplification stages, AGC and ADC have a strong effect on the pulse blanking circuitry implemented in the digital part of the receiver front-end. Careful design of the amplifiers able to recover quickly from the saturation condition as well as the AGC and the ADC schemes need to be provided in the future especially for those aviation receivers which will cope with such a pulsed interference environment.

In fact, the saturation status of the front-end increases the delay in the deactivation time of the blanker leading to the suppression of a portion of the useful signal. However, because of the presence of the tails, of the interfering pulse, it has been shown that, the de-activation time is not null.

It is important to remark that these results are strongly dependent on the Gaussian shape of DME/TACAN pulse. Moreover, these results are obtained for a determined pulsed interference scenario; possible interference scenarios stronger than those considered so far, may affect the active components of the receiver front-end differently, thus leading even to an increase of the cumulative recovery time needed to resume the nominal operational condition. Nevertheless, knowledge of the interfering scenario allows for the determination of an optimal range of the deactivation time which might be forced by the receiver manufacture.

As an alternative to this optimisation, innovative mitigation algorithms, independent from the receiver design and capable of extracting the interference component from the composite received signal, preserving as much as possible the useful GNSS signal energy, need to be investigated. In particular, in the last years, researchers have focused their attention on a new family of interference detection and mitigation algorithm based on a more sophisticated signal processing technique, as, for example, based on the use of a 2D transformation. In [16], an innovative interference mitigation algorithm based on the use of the wavelet transform is proposed against the composite DME/TACAN interference. The performance of such methods in suppressing the pulsed interference overperforms the results achieved through a traditional blanking operation at the expenses of an increased computational burden in the algorithm implementation.

8 References

1 Margaria, D., Fantino, M., Musumeci, L.: 'Acquisition and tracking of Galileo IOV E5 signals: experimental results and performance evaluation'. Proc. of European Navigation Conf. on GNSS, Gdanks, Poland, April 2012

2 Margaria, D., Nicola, M., Dovis, F., Linty, N., Musumeci, L.: 'Galileo in-orbit validation E1 and E5 signals'. Proc. of the Sixth ESA Workshop on Satellite Navigation Technologies and European Workshop on GNSS Signal and Signal Processing (NAVITEC), Noordiwijk, The Netherlands, December 2012

3 De Angelis, M., Fantacci, R., Menci, S., Rinaldi, C.: 'Analysis of air traffic control systems interference impact on Galileo aeronautics receivers'. Proc. of the 2005 National Technical Meeting of the Institute of Navigation, San Diego, CA, January 2005, pp. 346–357

4 Hegarty, T., Van Dierendonck, A.J., Bobyn, D., Tran, M., Kim, T., Grabowski, J.: 'Suppression of pulsed interference through blanking'. Proc. of the IAIN World Congress in association with the U.S. ION Annual Meeting, San Diego, CA, June 2000

5 Grabowski, J., Hegarty, T.: 'Characterization of L5 receiver performance using digital pulse blankin'. Proc. of the 15th Int. Technical Meeting of the Satellite Division of the Institute of Navigation (ION GPS 2002), Portland, OR, September 2002, pp. 1630–1635

6 ICAO.: 'Aeronautical Communications', Annex 10, Volume I

7 Bastide, F., Chatre, E., Macabiau, C., Roturier, B.: 'GPS L5 and GALILEO E5a/E5b signal-to-noise density ratio degradation due to DME/TACAN signals: simulations and theoretical derivations'. Proc. of the 2004 National Technical Meeting of the Institute of Navigation, San Diego, CA, January 2004, pp. 1049–1062

8 Erlandson, R.J., Kim, T., Hegarty, T., Van Dierendonck, A.J.: 'Pulsed RFI effects on aviation operation using GPS L5'. Proc. of the 2004 National Technical Meeting of the Institute of Navigation, San Diego, CA, January 2004

doi: 10.1049/iet-rsn.2013.0198

9 Gao, G.X.: 'DME/TACAN interference and its mitigation in L5/E5 bands'. Proc. of the 20th Int. Technical Meeting of the Satellite Division of The Institute of Navigation, Forth Worth, TX, September 2007, pp. 1191–1200
10 Anyaegbu, E., Brodin, G., Cooper, J., Aguado, E., Boussakta, S.: 'An integrated pulsed interference mitigation for GNSS receivers', *J. Navig.*, 2008, **61**, (2), pp. 239–255
11 RTCA DO-229D: 'Minimum Operational Performance Standards for Global Positioning System/Wide Area Augmentation System Airborne Equipment', 2006
12 RTCA DO-292: 'Assessment of Radio Frequency Interference Relevant to the GNSS L5/E5a Frequency Band', 2004
13 Soubielle, J., Vigneau, W., Samson, J., Banos, D.J., Musumeci, L.: 'Description of an interference test facility (ITF) to assess GNSS receivers performance in presence of interference'. Proc. of the Fifth ESA Workshop on Satellite Navigation Technologies and European Workshop on GNSS Signal and Signal Processing (NAVITEC), Noordiwijk, The Netherlands, December 2010
14 Borre, K., Akos, D.M., Bertelsen, N., Rinder, P., Jensen, S.H.: 'A software-defined GPS and Galileo receiver a single-frequency approach' (Birkhuser Boston) 2007
15 Fantino, M., Nicola, M., Molino, A.: 'N-Gene GNSS receiver: benefits of software radio in navigation'. Proc. of the European Navigation Conf. on GNSS, Naples, Italy, May 2009
16 Musumeci, L., Samson, J., Dovis, F.: 'Experimental assessment of distance measuring equipment and tactical air navigation interference on GPS L5 and Galileo E5a frequency bands'. Proc. of the 6th ESA Workshop on Satellite Navigation Technologies and European Workshop on GNSS Signal and Signal Processing (NAVITEC), Noordiwijk, The Netherlands, December 2012

doi: 10.1049/iet-rsn.2013.0198